PROCEEDINGS OF SCIENCE

Evaluation of the global magnetic noise for the stochastic gravitational wave background search

Tatsuki Washimi,[a,*] **Isamu Fukunaga,**[b] **Yousuke Itoh,**[b] **Nobuyuki Kanda,**[b] **Atsushi Nishizawa,**[c] **Jun'ichi Yokoyama**[c,d] **and Takaaki Yokozawa**[e]

[a] *Gravitational Wave Science Project (GWSP) Kamioka Branch, National Astronomical Observatory of Japan (NAOJ), Kamioka-cho, Hida City, Gifu 506-1205, Japan*

[b] *Department of Physics, Graduate School of Science, Osaka Metropolitan University, Sumiyoshi-ku, Osaka City, Osaka 558-8585, Japan*

[c] *Research Center for the Early Universe (RESCEU), The University of Tokyo, Bunkyo-ku, Tokyo 113-0033, Japan*

[d] *Department of Physics, The University of Tokyo, Bunkyo-ku, Tokyo 113-0033, Japan*

[e] *Institute for Cosmic Ray Research (ICRR) KAGRA Observatory, The University of Tokyo, Kamioka-cho, Hida City, Gifu 506-1205, Japan*

E-mail: tatsuki.washimi@nao.ac.jp

A stochastic gravitational wave background (SGWB) is a weak and persistent background of gravitational waves (GWs) and can provide valuable insights into the origins and evolution of the universe. To detect the SWGB, cross-correlations between multiple GW detectors are calculated and local noise is canceled; however, global coherent noises, such as the Schumann resonance, remain and affect the observation. The Schumann resonance is a natural phenomenon in which the Earth's electromagnetic field resonates at extremely low frequencies (ELF wave) of approximately 8, 14, 20 Hz, *etc.*This frequency range is similar to the wavelength of the Earth's circumference and is generated by the interaction of lightning discharges in the ionosphere and the Earth's surface. To evaluate the characteristics of the Schumann resonance, we have introduced a setup for Schumann resonance observations at the entrance of the KAGRA site and evaluate the temporal variation of the spectrum. Its effect on SGWB search based on our data is estimated using the Fisher matrix formalism.

38th International Cosmic Ray Conference (ICRC2023)
26 July - 3 August, 2023
Nagoya, Japan

*Speaker

PoS(ICRC2023)1561

1. Introduction

A gravitational wave (GW) is a wave of space–time distortion predicted using the general theory of relativity. The first direct detection of GWs was achieved by LIGO in the US (Hanford and Livingston) in 2015 [1], and more than 90 compact binary coalescence events were observed [2] by LIGO and Virgo in Italy [3]. KAGRA [4, 5] is a GW detector located underground in Kamioka, Japan. Its construction began in 2012, and an international joint observation was conducted in 2020 [6, 7]. A stochastic GW background (SGWB) is a random superposition of GWs from several black holes, the inflation of the Universe, etc., and is an extremely small and long-term signal. It has not yet been detected directly; however, pulsar timing array experiments such as EPTA+InPTA [8], NANOGrav [9], and PPTA [10] suggested an indirect SGWB signal at a frequency on the order of nano–Hz, recently. To detect an SGWB using ground-based interferometric GW detectors (LIGO, Virgo, KAGRA, and other detectors), the cross-correlation between multiple GW detectors is calculated and local noise is canceled; however, global coherent noise remains, which affects the observation.

The Schumann resonance [12, 13] is a natural phenomenon in which the Earth's electromagnetic field resonates between the ionosphere and the Earth's surface, at extremely low frequencies (ELF wave) approximately 8 Hz, 14 Hz, 20 Hz, *etc.*, which are generated by the interaction of lightning discharges. Schumann resonances generate correlated noise through instrumental magnetic couplings, which affects SGWB search [14, 15, 18]. Its effect on the parameter estimation for an SGWB was investigated by Mayers *et al.* [16] for a three-detector (HLV) case using Bayesian inference and byHimemoto *et al.* [20] for a four-detector case including KAGRA by the Fisher matrix formalism. These studies were based on magnetic fields and correlations measured at LIGO and Virgo [22], without consideration of their time variances. At the KAGRA site, short-time measurements (a few hours to two weeks) of the Schumann resonance were performed several times [5, 21, 22]; however, continuous observations are not available.

In this study, we introduce a setup for Schumann resonance observations at the entrance of the KAGRA site and evaluate the temporal variation in the spectrum. The effect of the temporal variation on SGWB search based on our data is estimated using Fisher matrix formalism.

2. Observation and modeling of global magnetic field

Continuous observations of the global magnetic field at the entrance of the KAGRA Tunnel commenced at the end of August 2022. The magnetometers used were Metronix MFS-06e [23] 1-axial induction coils operated with Metronix ADU-08e [24] and synchronized by a GPS clock. The observation period, sampling rate, and direction of the two horizontal magnetometers are summarized in Table 1. Herein, the data of "axis 2" in the second period is used for the following analysis.

Figure 1 (black) shows an example of the power spectral density (PSD) of the magnetic field for 1 h from 2023-05-05 to 10:00 UTC. The peaks of the Schumann resonance from the first to fourth modes are clearly indicated. To evaluate the spectral characteristics, a combination of the

Table 1: Observation period and the corresponding configurations.

Period		Sampling rate	Direction from North	
start	end		axis 1	axis 2
2022-08-26	2022-10-24	64 Hz	230°	110°
2022-10-24	2022-12-13	128 Hz	200°	110°
2023-05-04	continuing	256 Hz	200°	110°

Lorentzian functions

$$M(f) = \sum_{\ell=1}^{7} M_\ell(f) + M_{\mathrm{BG}}(f), \tag{1}$$

$$M_\ell(f) = \frac{A_\ell \cdot (f_\ell/2Q_\ell)^2}{(f - f_\ell)^2 + (f_\ell/2Q_\ell)^2}, \tag{2}$$

$$M_{\mathrm{BG}}(f) = A_{\mathrm{BG}} \cdot \left(\frac{f}{1\ \mathrm{Hz}}\right)^{-\alpha_{\mathrm{BG}}} + C_{\mathrm{BG}} + M_{\mathrm{AC}}(f) \tag{3}$$

is introduced with reference to studies pertaining to atmospheric physics [25–28]. Here, $M_\ell(f)$ is the PSDs, A_ℓ is the peak value, f_ℓ is the resonant frequency, Q_ℓ is the quality factor for the ℓ–th mode, and $M_{\mathrm{BG}}(f)$ represents the background component including some local noises (not the Schumann resonance). The result of a χ^2–fitting for the measured PSD using Eq. (1) is shown in Fig. 1 (red).

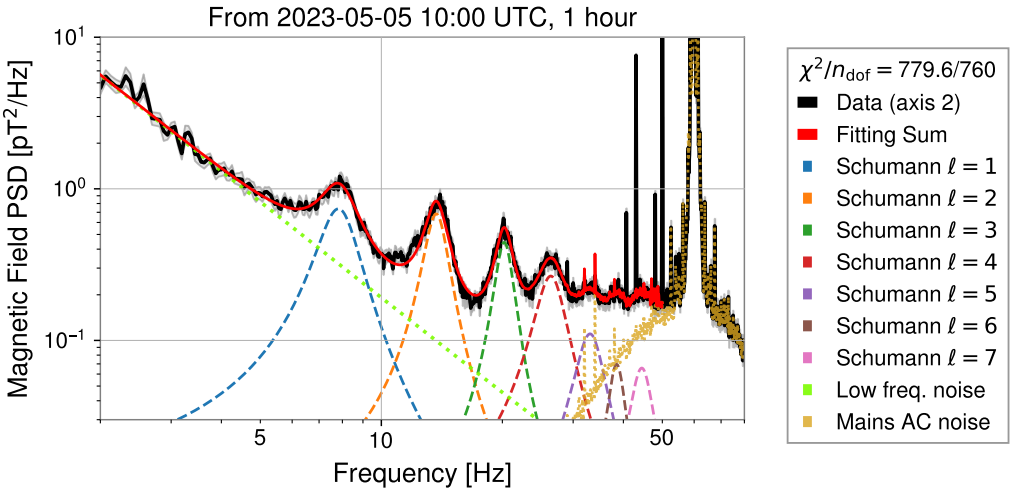

Figure 1: Example of a power spectral density (PSD) of magnetic field (axis 2) for 1 h from 2023-05-05 10:00 UTC. Black: observed data (median±4%); colors: fitting results.

The same procedures are performed for each hour using the observation data from May 4 to July 9, 2023. Figure 2 (top) shows the obtained Schumann resonance parameters $\{f_\ell, Q_\ell, A_\ell\}$ for every hour, which were averaged over the date because they have approximately 1 day period [26]. The PSDs of the Schumann resonance obtained using each parameter are shown in Fig. 2 (bottom). The dotted green line represents the PSD calculated using the mean values of each parameter.

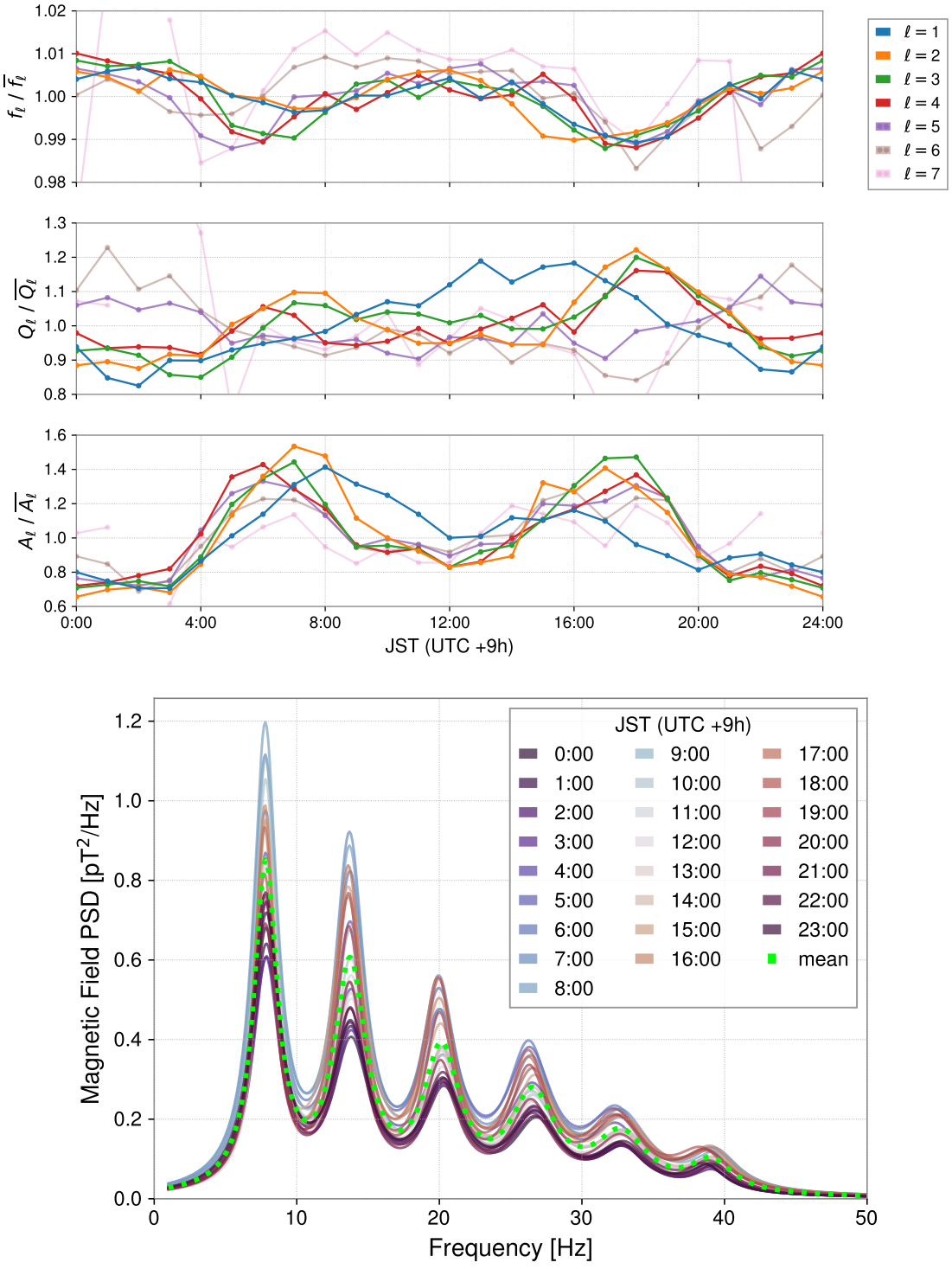

Figure 2: Top: Time variance of Schumann resonance parameters obtained every hour, which was averaged over the days from May 4 to July 9, 2023. Bottom: Power spectral densities (PSDs) of Schumann resonance every hour for each parameter.

3. Fisher analysis for stochastic gravitational-wave search

To verify the effect of the time variance of the Schumann resonance spectrum on SGWB search, Fisher analysis is performed based on the protocol of Himemoto *et al.* [20], where four GW detectors (LIGO Hanford, LIGO Livingston, Virgo, and KAGRA) and their corresponding design sensitivities were assumed. The cross-spectrum density (CSD) of the SGWB signal between the i–th and j–th GW detectors U_{ij}^{GW} can be expressed as

$$U_{ij}^{\mathrm{GW}}(f;\Omega_0,n_{\mathrm{GW}}) = \frac{3H_0^2}{10\pi^2}\frac{\Omega_{\mathrm{GW}}(f)}{f^3}\gamma_{ij}(f), \tag{4}$$

$$\Omega_{\mathrm{GW}}(f) = \Omega_0 \cdot \left(\frac{f}{25\mathrm{Hz}}\right)^{n_{\mathrm{GW}}}, \tag{5}$$

where f is the frequency, H_0 is the present Hubble parameter, and $\gamma_{ij}(f)$ is the overlap reduction function of the SGWB signal [29]. The GW parameters are set to$\Omega_0 = 3\times10^{-9}$ and $n_{\mathrm{GW}} = 2/3$ (astronomical sources) in this study. Meanwhile, the CSD of the global correlated magnetic noise U_{ij}^{GW} can be expressed as

$$U_{ij}^{\mathrm{Mag}}(f;\kappa_i,\kappa_j,\beta_i,\beta_j,\psi_i,\psi_j) = r_i(f)\cdot r_j(f)\cdot\sum_{\ell=1}^{6} M_\ell(f)\cdot\gamma_{ij,\ell}^{\mathrm{Mag}}(\psi_i,\psi_j), \tag{6}$$

$$r_i(f) = \left(\frac{\kappa_i}{10^{23}\ \mathrm{pT}}\right)\left(\frac{f}{10\ \mathrm{Hz}}\right)^{-\beta_i}, \tag{7}$$

where $r_i(f)$ is the coupling function from a magnetic field to a strain signal on the GW detector, and $\gamma_{ij,\ell}^{\mathrm{Mag}}(\psi_i,\psi_j)$ is the overlap reduction function for the ℓ–th mode of the Schumann resonance [18]. The seventh mode is disregarded in this analysis because it is small and its fitting uncertainty is significant. The magnetic coupling parameters $\{\kappa_i,\beta_i,\psi_i\}$ are set to the values listed in TABLE I of Ref. [20].

The Fisher matrix that accounts for the global correlated magnetic noise [20] is expressed as

$$F_{ab} = 2T_{\mathrm{obs}}\sum_{(i,j)}\int_{f_{min}}^{f_{max}}\frac{\partial_a U_{ij}\partial_b U_{ij}}{S_iS_j}df, \tag{8}$$

$$U_{ij}(f;\theta_a) = U_{ij}^{\mathrm{GW}}(f;\Omega_0,n_{\mathrm{GW}}) + U_{ij}^{\mathrm{Mag}}(f;\kappa_i,\kappa_j,\beta_i,\beta_j,\psi_i,\psi_j), \tag{9}$$

where T_{obs} is the observation time (set to 1 year in this study), and S_i is the sensitivity of the i–th GW detector (same as used in Ref. [20]). The statistical error of parameter θ_a is expressed as $\sigma_a = \sqrt{[F^{-1}]_{aa}}$. In this study, the parameter set is $\{\theta_a\} = \{\Omega_0, n_{\mathrm{GW}}, \kappa_i, \beta_i, \psi_i\}$. The magnetic field is assumed to be observed by magnetometers independently, and the Schumann resonance parameters $\{f_\ell, Q_\ell, A_\ell\}$ are not included in the Fisher matrix. Moreover, the systematic biases $\Delta\theta_a$ in the best-fit parameters from the actual values caused by overlooking the presence of a global

magnetic field are expressed as

$$\Delta\theta_a = \sum_b [\mathcal{F}^{-1}]_{ab}\, s_b, \tag{10}$$

$$\mathcal{F}_{ab} = 2T_{\rm obs} \sum_{(i,j)} \int_{f_{min}}^{f_{max}} \frac{\partial_a U_{ij}^{\rm GW} \partial_b U_{ij}^{\rm GW} - U_{ij}^{\rm Mag} \partial_a \partial_b U_{ij}^{\rm GW}}{S_i S_j} df, \tag{11}$$

$$s_b = 2T_{\rm obs} \sum_{(i,j)} \int_{f_{min}}^{f_{max}} \frac{U_{ij}^{\rm Mag} \partial_b U_{ij}^{\rm GW}}{S_i S_j} df. \tag{12}$$

The blue graphs in Fig. 3 show the results of Fisher analysis based on the stationary magnetic field using the Schumann resonance parameters, fixed at each time point or at the mean values (shown in Fig. 2). To consider the day modulation of the magnetic field, the observation time $T_{\rm obs}$ was partitioned into 24 segments, and the Fisher analysis was performed for each hour. Finally, their summations were obtained as follows:

$$F_{ab} = \sum_{n=0}^{23} \frac{1}{24} F_{ab}(t_n), \quad \mathcal{F}_{ab} = \sum_{n=0}^{23} \frac{1}{24} \mathcal{F}_{ab}(t_n), \quad s_b = \sum_{n=0}^{23} \frac{1}{24} s_b(t_n). \tag{13}$$

The orange graphs in Fig. 3 show the results for the time-varying case. The errors for the GW parameters are smaller and the biases are similar, compared to those for the stationary magnetic field case based on fixed mean values of the Schumann resonance parameters.

4. Summary and prospects

In this study, we performed a continuous observation of a magnetic field at the entrance of the KAGRA tunnel and characterized the time variance of the Schumann resonance. The effect of the global magnetic noise on SGWB search was evaluated via Fisher analysis based on the observed magnetic field. We discovered that the errors for the GW parameters were smaller and the biases were similar to those for the stationary magnetic field case with fixed mean values of the Schumann resonance parameters.

In the future, longer-term observational data will be used. Investigations into the directional information of the magnetic field vector are essential, and the overlap reduction function of the magnetic noise from a theoretical model can be replaced with observational data, owing to its time variance. Magnetic coupling to the GW channel should be measured for KAGRA via an injection test and applied to the Fisher analysis.

References

[1] B. P. Abbott *et al.*(The LIGO Scientific Collaboration and The Virgo Collaboration), Phys. Rev. Lett. 116, 061102 (2016).

[2] https://arxiv.org/abs/2111.03606

[3] F. Acernese *et al.*, 2015 Class. Quantum Grav. 32 024001.

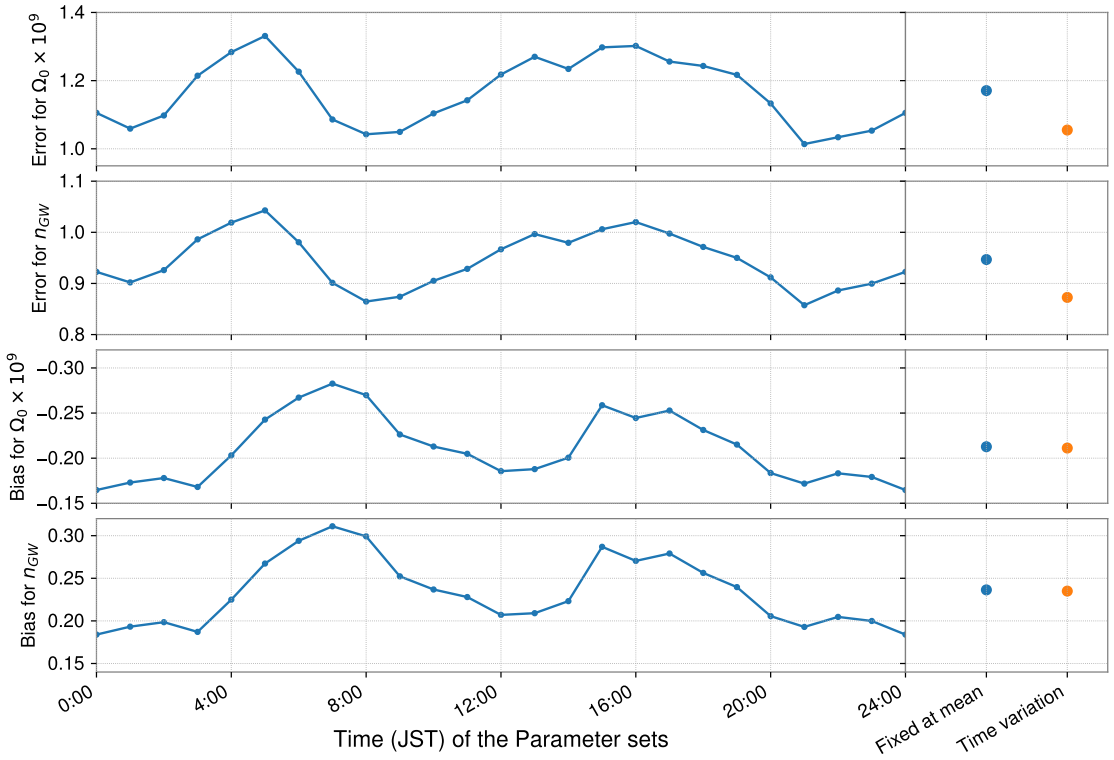

Figure 3: Statistical errors and systematic biases for SGWB parameters evaluated via Fisher analysis. Blue: Based on the stationary magnetic field using Schumann resonance parameters fixed at each time or mean value. Orange: Based on the magnetic field and considering the time variance of Schumann resonance parameters.

[4] T. Akutsu *et al.*, (KAGRA collaboration), PTEP 2021, 5, 05A101.

[5] H. Abe *et al.*(The KAGRA collaboration), Galaxies 2022, 10(3), 63.

[6] R. Abbott *et al.*(The LIGO Scientific Collaboration, The Virgo Collaboration, The KAGRA Collaboration), PTEP 2022, 6, 063F01.

[7] H. Abe *et al.*(The KAGRA collaboration), PTEP 2022, ptac093.

[8] https://arxiv.org/abs/2306.16214

[9] G. Agazie *et al.*, 2023 ApJL 951 L8.

[10] D. J. Reardon *et al.*, 2023 ApJL 951 L6.

[11] H. Xu *et al.*, 2023 Res. Astron. Astrophys. 23 075024.

[12] W. O. Schumann, Z. Naturforsch. Teil A 7, 149 (1952).

[13] W. O. Schumann, Z. Naturforsch. Teil A 7, 250 (1952).

[14] N. Christensen, Phys. Rev. D 46, 5250 (1992).

[15] B. Allen and J. D. Romano, Phys. Rev. D 59, 102001 (1999).

[16] P. M. Meyers, K. Martinovic, N. Christensen, and M. Sakellariadou, Phys. Rev. D 102, 102005 (2020) .

[17] E. Thrane, N. Christensen, and R. M. S. Schofield, Phys. Rev. D 87, 123009 (2013).

[18] Y. Himemoto and A. Taruya, Phys. Rev. D 96, 022004 (2017).

[19] Y. Himemoto and A. Taruya, Phys. Rev. D 100, 082001 (2019).

[20] Y. Himemoto, A. Nishizawa, and A. Taruya, Phys. Rev. D 107, 064055 (2023).

[21] S. Atsuta *et al.*, 2016 J. Phys.: Conf. Ser. 716 012020.

[22] M. W. Coughlin *et al.*, Phys. Rev. D 97, 102007 (2018).

[23] https://www.metronix.de/metronixweb/en/geophysics/products/sensors/mfs-06e/

[24] https://www.metronix.de/metronixweb/en/geophysics/products/logger/adu-08e/

[25] D. D. Sentman, Radio Science 22, 4, 595-606, July-August 1987.

[26] C, Price, A. Melnikov, J. Atmos. Sol. Terr. Phys. 66, 13–14, (2004), 1179-1185.

[27] Y. Tulunay *et al.*, J. Atmos. Sol. Terr. Phys. 70, 2–4, (2008), 669-674.

[28] E. R. Williams, V. C. Mushtak, A. P. Nickolaenko, J. Geophys. Res., 111, D16107 (2006).

[29] Atsushi Nishizawa, Atsushi Taruya, Kazuhiro Hayama, Seiji Kawamura, and Masa-aki Sakagami, Phys. Rev. D 79, 082002 (2009).